Title: Investigation of Postmenopausal Alteration of Trabecular Structure on Calcaneus Radiographs Using Various Fractal Analysis Methods

Author: H. Jelinek, I. Stefan, R. Badea and A. Prie
Author Address: hjelinek@csu.edu.au

Conference Title: Year of Conference: 2007
Conference Location: Iasi, Romania
Editor: Publisher: IEEE Press
URL: http://scs.etc.tuiasi.ro/isscs2007/

Abstract: Four different methods of fractal analysis able to analyse grayscale images were applied to trabecular structure of the calcaneus, as it appears on the plain lateral radiograph. Their capacity to recognize a radiograph as belonging to a pre- or postmenopausal group was investigated. The study used 3 different regions of interest (ROI), after digital processing. Two-tailed p-value was calculated to compare the results. K-means clustering, nearest neighbour (1-nn) and 3-nearest neighbour (3-nn) algorithms ' were used to objectively assess the ability of these analysis methods to discriminate the two sets of radiographs. Using these methods, 19 out of 24 X-rays were correctly classified (p = 0.004).

CSU ID: CSU285406

Investigation of postmenopausal alteration of trabecular structure on calcaneus radiographs using various fractal analysis methods

I. Stefan [1], C. Vertan [2], H.F. Jelinek [3], R. Badea [4], A. Prie [1]
[1] Emergency County Hospital, Traumatology Department, Baia Mare, Romania
IonStefan@gmx.net
[2]Image Processing and Analysis Laboratory, "Politehnica" University, Bucharest
[3] School of Community Health, Charles Sturt University, Australia
[4] University of Medicine and Pharmacy "Iuliu Hatieganu" Cluj-Napoca, Medical Imagery Dept., Romania

***Abstract*— Four different methods of fractal analysis able to analyze grayscale images were applied to trabecular structure of the calcaneus, as it appears on the plain lateral radiograph. Their capacity to recognize a radiograph as belonging to a pre- or postmenopausal group was investigated. The study used 3 different regions of interest (ROI), after digital processing. Two-tailed p-value was calculated to compare the results. K-means clustering, nearest neighbor (1-nn) and 3-nearest neighbor (3-nn) algorithms – were used to objectively assess the ability of these analysis methods to discriminate the two sets of radiographs. Using these methods, 19 out of 24 X-rays were correctly classified (p = 0.004).**

Introduction

Bone strength is determined by bone mineral density (BMD) and bone quality [1]. After the limits of BMD to assess risk fracture became apparent, factors defining bone quality, such as bone size, accumulation of microdamage, subclinical osteomalacia, bone microstructure and geometric characteristics, drew their share of attention [2]. Trabecular architecture is accepted as one of the main factors defining bone quality [3]. Three-dimensional trabecular architecture can now be assessed using high-resolution digital imaging techniques such as high-resolution magnetic resonance (hrMR) and micromagnetic resonance (micro-MR), high-resolution computed tomography (hrCT), as well as micro-computed tomography (microCT). Along with these highly sophisticated imaging techniques, computerized analysis of radiographic patterns of trabecular bone still constitutes a valid field of research[4],[5].

During the accelerated phase of postmenopausal bone loss, women lose 25% of trabecular bone [6]. Trabecular architecture suffers dramatic changes in terms of a decrease in connectivity, thinning, perforation or loss of trabeculae [7].

The aim of the present work is to determine if fractal analysis applied to trabecular texture, as it appears on the plain lateral radiograph of the calcaneus can be used to identify postmenopausal alteration of trabecular structure and eventually to classify X-rays as belonging to a pre- or postmenopausal group.

Given the grave consequences of osteoporosis, any automated method able to detect subtle changes of the trabecular texture accompanying this process could be important to early recognition and improved therapy outcomes. If inexpensive radiographs obtained during routine clinical practice for trauma of the foot or ankle or complaints associated with other diseases, could prove to be the source of such information, this would provide a more accessible and cheap tool in the hand of medical staff.

Materials and methods

We analyzed 2 sets of 12 radiographs from two groups of women: a premenopausal group between 26 and 38 years (yrs) (mean age = 33 yrs, standard deviation = 3,8 yrs) and a postmenopausal group with ages between 48 and 65 yrs (mean age = 56 yrs, standard deviation = 5,5 yrs).

Radiographs were digitized using a 2.0 Mpixel Fuji FinePix 2600 Zoom camera and grayscale images obtained using a public domain programme from the National Institutes of Health, ImageJ (http://rsb.info.nih.gov/ij/). Three 150/150 pixels regions of interest (ROI) were selected on each X-ray. ROI 0 corresponds to the thalamic region, ROI 1 to Ward's triangle and ROI 2 to the region where the posterior plantar group of trabeculae intersects the thalamic group, Fig. 1.

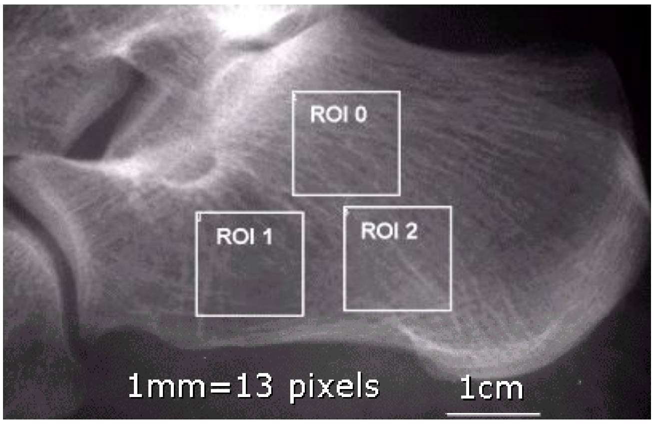

Figure 1. The three ROIs analyzed on each X-ray

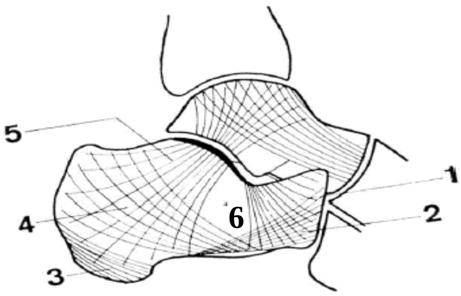

Figure 2. Trabecular systems within the calcaneus bone: anterior apophysis system (1), plantar system (2, 4), achillean system (3), thalamic system (5) and Ward triangle (6).

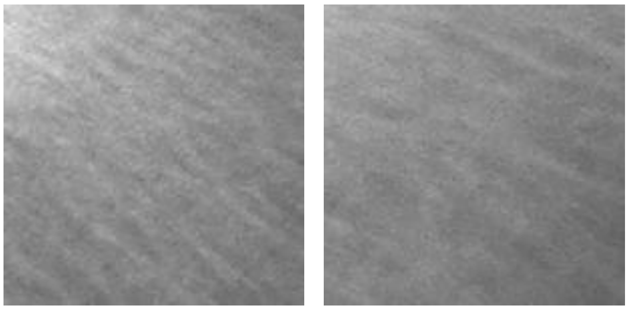

Figure 3. Image of ROI 0, corresponding to thalamic area from premenopausal group (left image) and postmenopausal group (right image)

Classical description of trabecular systems of calcaneum [8], Fig. 2, was used as a guide to select "significant" ROI. As a result, ROI 1 corresponds to compressive stress trajectories, ROI 2 corresponds to compressive and tensile stress trajectories. ROI 2 coresponds to a minimum of compressive and tensile stresses.

For the fractal analysis we used Gwyddion (http://gwyddion.net/). Gwyddion is a free software, covered by GNU General Public License. It provides 4 different methods of fractal analysis: cube counting method (fdcc), triangulation method (fdt), the variance method (fdv) and power spectrum method (fdps). Images represented by ROI are analysed as grayscale images. This could be an advantage in this specific case, as no information is lost through a binarization procedure.

The results for the 2 sets of X-rays were compared for corresponding ROI, Fig. 3, and fractal analysis method. We used unpaired t-test to calculate the two-tailed p-value to estimate statistical significance of differences between these results.

Using computed fractal dimensions as attributes, we made an attempt to classify the X-rays and to determine the ability of these fractal analysis methods to discriminate between the two sets of radiographs. For this purpose, two instance-based learning algorithms – nearest neighbor (1-nn) and 3-nearest neighbor (3-nn) – were used. The 2 sets of 12 radiographs represented the training set for the 1-nn and 3-nn algorithms, with membership of each X-ray image to one of the two sets known. Successively, each X-ray was considered a new, unknown object and was classified using the k-nn algorithm applied to the remaining 23 radiographs (leave-one-out algorithm). If the X-ray was classified to the set which it belonged to, the classification was correct. Otherwise, it was considered an error.

RESULTS

All calculated fractal dimensions are presented in Tables 1, 2, 3, 4, 5 and 6. Results of differences between the regions of interest and fractal analysis methods in terms of pre- and postmenopausal groups are represented in Table 7.

K-nn algorithms rendered a minimum number of 5 errors, in two instances: using 3-nn on 3 parameters, fdps, fdv and fdt calculated for ROI 1 and using 3-nn on 2 parameters, fdps and fdv calculated for ROI 1. K-means clustering algorithm also rendered a minimum number of 5 errors, in one instance, for ROI 2, characterized by the parameters fdps and fdt, Fig. 4, Fig. 5.

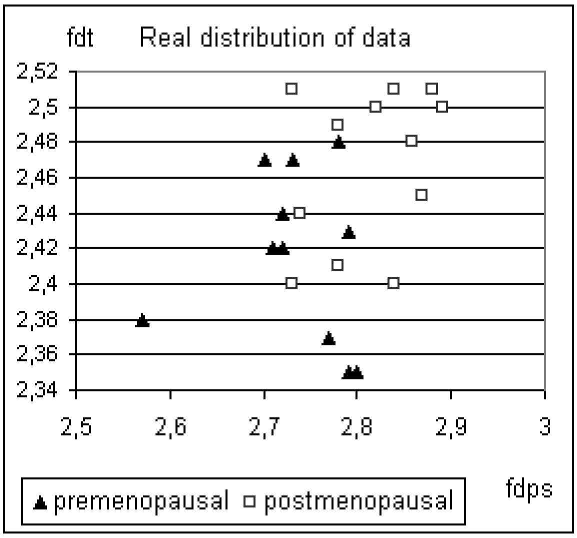

Figure 4. ROI 2 from each X-ray characterized by fdps and fdt

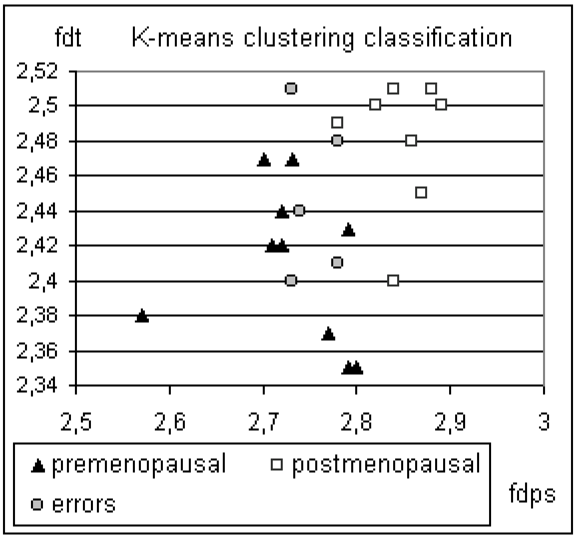

Figure 5. Same data as in Fig. 4 after k-means clustering.

Discussion and conclusions

Fractal analysis applied to trabecular texture of calcaneus on radiographs has led to interesting findings in previous studies. Significant statistical differences were found between postmenopausal women with osteoporotic (OP) vertebral crush fractures and age-matched control group [9] and also found between vertebral, hip, and wrist fracture cases and control groups in postmenopausal women [10]. Less significant correlation was found with bone strength [11]. A significant relationship between the fractal Hmean parameter and structural histomorphometric indices was also reported [12].

In our study, we could demonstrate that results from three out of four fractal analysis methods obtained statistically significant differences between the 2 groups of radiographs, for one or more ROI. Of interest is that the fourth fractal analysis method, fdv, contributed to the classifications (3-nn), which rendered minimum number of errors. Statistical significant differences did not necessarily led to the best classification results. Power spectrum method yielded statistically significant different results for all ROI, proving to be the most successful method from this point of view. Also three out of four fractal analysis methods yielded statistically significant different results from ROI 2.

Using k-nn and k-means clustering algorithms, 19 out of 24 X-rays (80%) were correctly classified ($X^2_{1,24} = 8.16$, $p = 0.004$).

Analysing multiple ROI proved to be helpful. More information could be extracted and processed, reflecting perhaps the heterogenity of trabecular structure. There is a striking correspondence between classical description of trabecular systems of calcaneus on sagittal anatomical sections and on lateral X-ray, which guided our ROI selection, and more recently described trajectories of principal stresses during gait evaluated on a finite element model of the foot [13].

For all 12 comparable sets of values (four fractal analysis methods and three ROI), the average values of fractal dimensions were higher for the postmenopausal group. The difference was significant in 2 instances: for the fdt method from ROI 2 (p=0.0124) and for the fdcc method from ROI 2 (p=0.015) and very significant in the other three instances, for the fdps method from ROI 0 (p=0.0069), the fdps method from ROI 1 (p=0.0088) and the fdps method from ROI 2 (p=0.004).

In a previous study [14] performed on the same X-rays and ROI, the box-counting fractal dimension (bcfd) was determined from binarized images with a dynamic thresholding technique. An identical k-nn classification algorithm rendered a minimum number of errors, 6, for two instances: 1-nn for the bcfd method from ROI 1 and ROI 2; 1-nn for the bcfd method from ROI 0,1 and 2. So, we can report a slightly lower number of errors with the present methods with an 5% improvement in accuracy.

Using the available 24 X-ray training set, new X-rays can be classified using the same k-nn and k-means clustering algorithms. In fact, the whole algorithm - from acquisition of the image to its classification - can be fully automated and eventually applied for the study of other sets of radiographs separated by other criteria (sex, BMD, presence of osteoporotic fracture, etc.).

References

[1] N.B. Watts, "Bone quality: getting closer to a definition.", J Bone Miner Res 2002, 17, pp.1148 –1150.

[2] S. Boonen, P. Nicholson, "Assessment of femoral bone fragility and fracture risk by ultrasonic measurements at the calcaneus." Age Ageing. 1998, 27(2), pp. 231-237.

[3] M.L.Bouxsein, "Mechanisms of osteoporosis therapy: a bone strength perspective." Clin Cornerstone, 2003, Suppl 2, pp.13-21.

[4] T.M. Link, S. Majumdar, "Current diagnostic techniques in the evaluation of bone architecture", Curr Osteoporos Rep, 2004, 2, pp. 47-52.

[5] L. Apostol, V. Boudousq, O. Basset, C. Odet, S. Yot, J. Tabary, J.M. Dinten, E. Boller, P.O. Kotzki and F. Peyrin. Relevance of 2D radiographic texture analysis for the assessment of 3D bone micro-architecture. Med Phys, 33(9), pp: 3546-3556, 2006.

[6] D. L. Hurley, S. Khosla, "Update on Primary Osteoporosis", Mayo Clin Proc. 1997;72, pp: 943-949.

[7] E. Seeman, "Reduced bone formation and increased bone resorption: rational targets for the treatment of osteoporosis", Osteopor. Int.,volume 14, Supplement 3, March, 2003.

[8] N. Burghele, "Fracturile calcaneului", Ed. Medicala, Bucuresti, 1978, pp. 15

[9] L. Pothuaud, E. Lespessailles, R. Harba, R. Jennane, V. Royant, E. Eynard, C. L. Benhamou, "Fractal Analysis of Trabecular Bone Texture on Radiographs: Discriminant Value in Postmenopausal Osteoporosis", Osteopor. Int., 1998, vol. 8, no.6, pp. 618-625.

[10] C.L. Benhamou, S.Poupon, E. Lespessailles, S. Loiseau, R. Jennane, V. Siroux, , et al., "Fractal analysis of radiographic trabecular bone texture and bone mineral density: two complementary parameters related to osteoporotic fractures", J Bone Miner Res. 2001 Apr;16(4), pp. 697-704.

[11] E. Lespessailles, A. Jullien, E. Eynard, R. Harba, G. Jacquet, J.P. Ildefonse,et al., Biomechanical properties of human os calcanei: relationships with bone density and fractal evaluation of bone microarchitecture. J Biomech. 1998, 31(9), pp. 817-824.

[12] E. Lespessailles, J. P. Roux, C. L. Benhamou, M. E. Arlot, E. Eynard, R. Harba, et al. "Fractal Analysis of Bone Texture on Os Calcis Radiographs Compared with Trabecular Microarchitecture Analyzed by Histomorphometry", Calcif Tissue Int. 1998, 63(2), pp. 121-125.

[13] V.L. Giddings, G. S. Beaupre´, R. T. Whalen, and D. R. Carter, "Calcaneal loading during walking and running", Med. Sci. Sports Exerc., 2000, 32(3), pp. 627–634.

[14] Stefan I., Prie A., Badea R., Vertan C., Assessment of age related changes in trabecular bone structure of calcaneus using fractal analysis (II), Abstr. in: Abstracts Book, National Conference SOROT, 14 –15 October 2004, Bucharest.

TABLE I. FRACTAL DIMENSIONS FOR ROI 0 OF THE PREMENOPAUSAL GROUP

Xray	1	2	3	4	5	6	7	8	9	10	11	12
fdv	2.67	2.67	2.68	2.62	2.67	2.59	2.68	2.69	2.64	2.69	2.69	2.66
fdcc	2.36	2.34	2.36	2.37	2.38	2.32	2.38	2.36	2.38	2.35	2.39	2.33
fdt	2.39	2.36	2.38	2.34	2.40	2.31	2.39	2.38	2.37	2.39	2.41	2.35
fdps	2.74	2.68	2.77	2.77	2.84	2.75	2.74	2.81	2.74	2.66	2.77	2.60

TABLE II. FRACTAL DIMENSIONS FOR ROI 0 OF THE POSTMENOPAUSAL GROUP

Xray	13	14	15	16	17	18	19	20	21	22	23	24
fdv	2.72	2.71	2.62	2.71	2.70	2.76	2.64	2.69	2.72	2.73	2.69	2.57
fdcc	2.40	2.39	2.33	2.36	2.40	2.40	2.37	2.37	2.40	2.40	2.36	2.33
fdt	2.43	2.40	2.33	2.29	2.41	2.42	2.36	2.38	2.43	2.42	2.38	2.30
fdps	2.75	2.83	2.77	2.81	2.83	2.87	2.78	2.89	2.81	2.83	2.76	2.76

TABLE III. FRACTAL DIMENSIONS FOR ROI 1 OF THE PREMENOPAUSAL GROUP

Xray	1	2	3	4	5	6	7	8	9	10	11	12
fdv	2,73	2,58	2.70	2,57	2.69	2.69	2,71	2.71	2.69	2,50	2,59	2,53
fdcc	2.40	2,32	2,40	2,32	2,39	2,38	2,39	2,40	2,37	2,32	2,32	2,31
fdt	2,47	2,33	2,43	2,32	2,41	2,42	2,38	2,43	2,42	2,32	2,34	2,36
fdps	2,75	2,63	2,76	2,66	2,78	2,73	2,77	2,79	2,71	2,58	2,64	2,46

TABLE IV. FRACTAL DIMENSIONS FOR ROI 1 OF THE POSTMENOPAUSAL GROUP

Xray	13	14	15	16	17	18	19	20	21	22	23	24
fdv	2.75	2.72	2.63	2.61	2.72	2.68	2.58	2.65	2.70	2.64	2.70	2.60
fdcc	2.45	2.41	2.37	2.31	2.38	2.41	2.35	2.38	2.42	2.36	2.39	2.38
fdt	2.51	2.45	2.39	2.31	2.42	2.46	2.37	2.39	2.46	2.35	2.40	2.41
fdps	2.72	2.80	2.70	2.70	2.85	2.81	2.75	2.83	2.81	2.82	2.77	2.81

TABLE V. FRACTAL DIMENSIONS FOR ROI 2 OF THE PREMENOPAUSAL GROUP

Xray	1	2	3	4	5	6	7	8	9	10	11	12
fdv	2.76	2.75	2.80	2.72	2.77	2.78	2.72	2.79	2.77	2.73	2.77	2.74
fdcc	2.38	2.38	2.44	2.38	2.41	2.35	2.37	2.32	2.41	2.41	2.40	2.35
fdt	2.42	2.42	2.48	2.42	2.43	2.35	2.37	2.35	2.47	2.47	2.44	2.38
fdps	2.72	2.72	2.78	2.71	2.79	2.79	2.77	2.80	2.73	2.70	2.72	2.57

TABLE VI. FRACTAL DIMENSIONS FOR ROI 2 OF THE POSTMENOPAUSAL GROUP

Xray	13	14	15	16	17	18	19	20	21	22	23	24
fdv	2.76	2.82	2.76	2.79	2.83	2.75	2.68	2.76	2.78	2.74	2.73	2.78
fdcc	2.45	2.48	2.38	2.35	2.44	2.41	2.39	2.45	2.45	2.44	2.38	2.45
fdt	2.51	2.51	2.41	2.40	2.48	2.45	2.44	2.50	2.51	2.49	2.40	2.50
fdps	2.73	2.88	2.78	2.84	2.86	2.87	2.74	2.89	2.84	2.78	2.73	2.82

TABLE VII. P-VALUES FOR EACH FRACTAL ANALYSIS METHOD AND EACH ROI

p-value	ROI 0	ROI 1	ROI 2
fdps	0.0069	0.0088	0.0040
fdt	0.6890	0.2741	0.0124
fdcc	0.1267	0.1254	0.0150
fdv	0.1597	0.3983	0.6343